

Ordered H₂O Structures on a Weakly Interacting Surface: A Helium Diffraction Study of H₂O/Au(111)

Gefen Corem,^{‡,‡} Pepijn R. Kole,^{‡,§,||} Jianding Zhu,^{||} Tatyana Kravchuk,[‡] J. R. Manson,[⊥] and Gil Alexandrowicz^{*,‡}

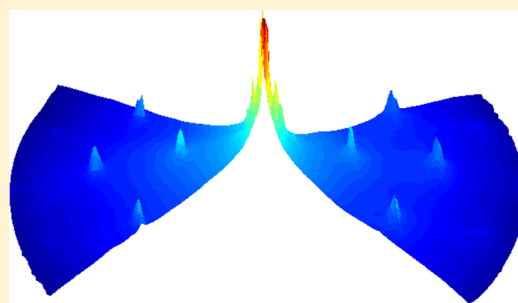
[‡]Schulich Faculty of Chemistry, Technion - Israel Institute of Technology, Haifa 32000, Israel

^{||}The Cavendish Laboratory, J. J. Thomson Avenue, Cambridge, CB3 0HE, United Kingdom

[⊥]Department of Physics and Astronomy, Clemson University, Clemson, South Carolina 29634, United States

S Supporting Information

ABSTRACT: In this manuscript we report helium atom scattering (HAS) measurements of the structure of the first H₂O layer on Au(111). The interaction between H₂O and Au(111) is believed to be particularly weak, and conflicting evidence from several indirect studies has suggested that water either grows as 3D ice crystals or as an amorphous wetting layer. In contrast, our measurements show that between 110 and 130 K, H₂O grows as highly commensurate well-ordered islands that only partially wet the gold surface. The islands produce a clear ($\sqrt{3} \times \sqrt{3}$)R30° diffraction pattern and are characterized by a well-defined height of ~ 5 Å with respect to the surface gold atoms. These findings provide support for a unique “double bi-layer” model, which has recently been suggested for this surface.



INTRODUCTION

In recent decades, numerous experimental and theoretical studies have been devoted to understanding the interaction of H₂O with metallic surfaces.^{1–3} This ongoing activity can be related to numerous technological applications and the significant experimental and theoretical challenges encountered when studying these delicate and complex surface systems. In particular, the sensitivity of H₂O molecules to electrons and radiation, the strong dependency of the observed structures on the exact preparation conditions, and the difficulties encountered in theoretical studies have led to conflicting results and controversy.^{1,2,4,5}

An experimental method that played a leading role in determining the structure of water layers on metal surfaces is low energy electron diffraction (LEED).^{1,2} While this technique has and is still supplying valuable information, it has a few limitations, in particular, the sensitivity of water surfaces to electron-induced damage and the lack of sensitivity to the positions of the protons within the layer, that is, the molecular orientation of water. Significant progress has been made in recent years by combining state-of-the-art scanning tunneling microscopy (STM) and theoretical calculations (e.g., refs 3, 6, and 7), a powerful combination that enables studying surfaces in real space and time. Real space techniques provide a major advantage when dealing with heterogeneous systems where the spatial averaging of diffraction techniques may lead to erroneous interpretation. On the other hand, STM studies of water surfaces are typically limited to ultralow temperatures where the dynamics are extremely slow. Furthermore, stringent limitations on the scanning parameters are required to avoid

significant perturbation effects, restricting these studies in terms of layer thickness, spatial resolution, and the ability to relate apparent height to the real height.^{6,8}

In this manuscript, we report helium atom scattering (HAS) measurements from an H₂O overlayer adsorbed on an Au(111) surface. While HAS measures in reciprocal space, which can complicate the structure analysis, especially on heterogeneous surfaces, it is an extremely nonperturbative technique, it is potentially very sensitive to light atoms, that is, the proton order in a water layer (this topic will be discussed in more detail below), and it is capable of measuring the average structure on an atomic scale even in the presence of significant thermal motion. These properties make HAS particularly suitable for measuring H₂O surface structures at elevated temperatures, as has been demonstrated in the past, for example, refs 9–12.

The Au(111) surface is believed to be characterized by a particularly weak H₂O–metal interaction, weaker than that of all the other close-packed noble and transition metals.^{13,14} STM measurements at low temperatures and coverages have shown that H₂O molecules predominantly populate the elbows of the herringbone reconstruction.⁸ Isothermal desorption experiments suggested that water does not wet the Au(111) surface and that 3D growth of H₂O takes place.¹⁵ However, a couple of STM studies have since indicated the formation of a first layer, which serves as a precursor to the growth of the subsequent layers.^{16,17} Furthermore, recent EELS measurements performed

Received: May 23, 2013

Revised: October 10, 2013

Published: October 10, 2013

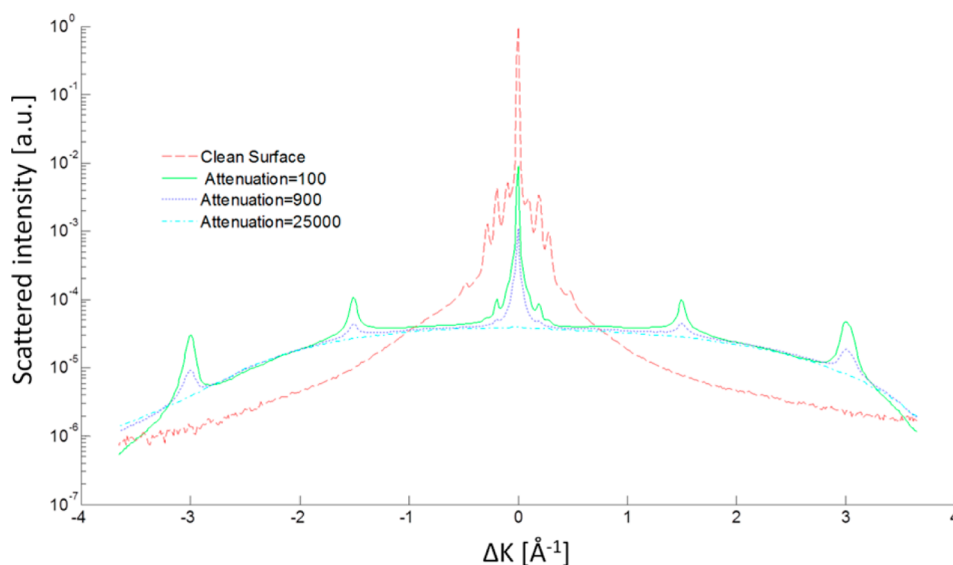


Figure 1. Angular scans measured at 110 K along the $\langle 110 \rangle$ crystal azimuth using an 8 meV ^3He beam. The measurements show the evolution of the angular distribution with increasing doses of H_2O , from a clean Au(111) surface (red dashed line), through an ordered H_2O overlayer (green full line, and blue dotted line) and up to what seems like an amorphous film of H_2O (dash-dot cyan line), obtained after substantial H_2O exposure (>10 L).

at 130 K were also interpreted as indicating spread out ice layers¹⁸ rather than 3D growth.

The current knowledge about the atomic-scale structure of the first layer of H_2O on Au(111) is rather limited. Ikemiya and Gewirth performed STM measurements at 100 K and concluded that the first layer of H_2O on Au(111) is amorphous.¹⁶ In contrast, a $(\sqrt{3} \times \sqrt{3})R30^\circ$ LEED pattern was reported by Pirug and Bonzel after dosing H_2O at 120 K.¹⁹

It should be noted that $(\sqrt{3} \times \sqrt{3})R30^\circ$ patterns, expected from the classical hexagonal bilayer model, were measured on several close-packed metal surfaces,¹ however, some of these findings have later been related to the perturbation effects of the experimental techniques used.^{2,3} One relatively recent example is water on Pt(111) where previous work has identified $(\sqrt{3} \times \sqrt{3})R30^\circ$ structures;²⁰ however, more recent STM experiments^{21,22} observe large unit cells and complex structures, consistent with HAS diffraction measurements.⁹ In fact, during the last two decades, experiments have detected a wealth of complex 1D, 2D, and 3D water structures on metals as opposed to the expected classic bilayer structures, raising doubts whether the hexagonal bilayer model for water, which was so widely embraced in the past, is applicable to any H_2O /pure-metal surface.^{4,23}

In a recent combined STM, infrared adsorption spectroscopy (IRAS), and density functional theory (DFT) study, Stacchiola et al. studied the growth of the first H_2O layer on Au(111) at 20 and 100 K.¹⁷ Restrictions on the spatial resolution excluded direct measurements of the atomic scale structure or its symmetry, however, by combining STM apparent height measurements, DFT calculations, and IRAS measurements, the authors concluded that the first layer of H_2O on Au(111) is a unique double-bilayer, that is, two traditional proton ordered water bilayers, one with a H-up and one with H-down stacked on top of each other. A schematic of the structure suggested by Stacchiola et al. is shown in the Supporting Information. At elevated temperatures of ~ 100 K, the STM measurements were too blurry to analyze; however, measurements at 20 K of films grown at 120 K provided some insight, showing rather large

islands (tens of nanometers large) that seem to nucleate at step edges.

■ EXPERIMENTAL SECTION

The measurements presented below were performed using the Cambridge helium spin echo (HeSE) spectrometer²⁴ and a new HeSE instrument that is being constructed at the Technion. A description of the scattering parameters of the Technion setup which are relevant to this study can be found in the Supporting Information. Both of these instruments were designed to perform ultrahigh energy resolution measurements of surface dynamics,²⁵ but were used in this study as fixed scattering geometry helium diffractometers with a 45° total scattering angle (using ^3He at Cambridge and ^4He at the Technion). Two Au(111) samples (Surface Preparation Lab, The Netherlands) were used in this study, both of which were aligned to within 0.1° and polished to a $0.03 \mu\text{m}$ roughness. The crystals were cleaned in situ by repeated cycles of Ar^+ sputtering (0.8 kV) and annealing at 800 K until no further improvements in the helium specular reflectivity were observed. Reflectivity values $>15\%$ were used as an indication for a clean and well ordered surface. Double-distilled water was thoroughly degassed using freeze–pump–thaw cycles and was deposited on the surface using two different dosing methods: (1) a capillary array doser was located 15 cm from the sample²⁶ and (2) background gas was deposited from a leak valve. We have also varied the deposition flux between ~ 0.4 to 1 L/min (where L denotes Langmuir = 10^{-6} Torr-sec), however, the diffraction data presented below did not seem to depend on any of these different deposition methods. The sample temperature was controlled using a liquid nitrogen coldfinger and a filament located behind the sample holder. To ensure that the water layer did not suffer any electron damage due to thermionic emission, we repeated the experiments while floating the sample at a negative potential (-50 V) but did not observe any changes in the experimental results.

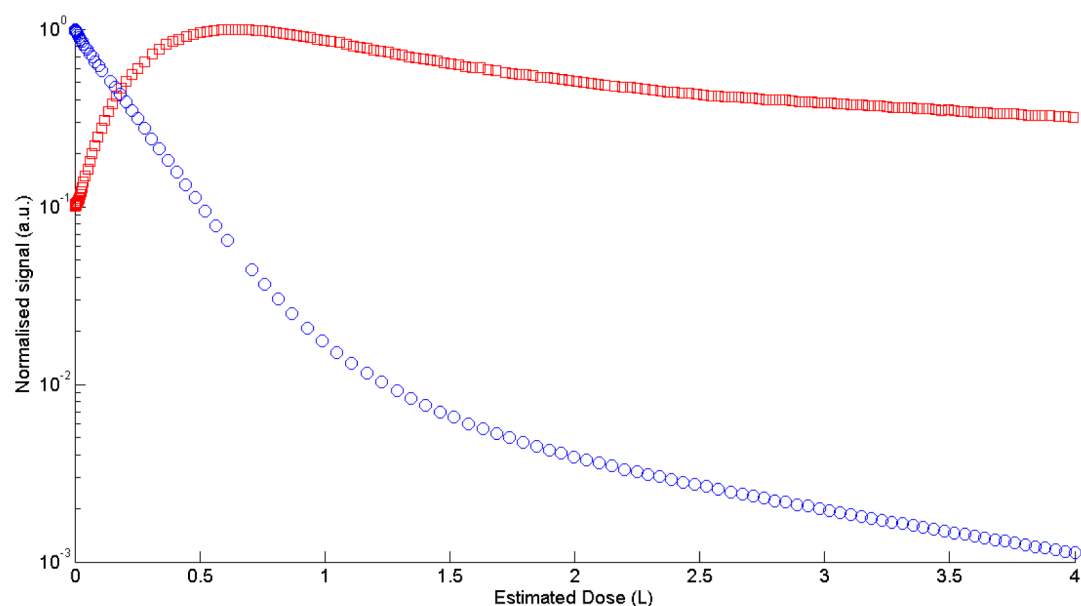


Figure 2. Evolution of the scattered helium intensity as a function of H₂O exposure measured at 110 K. The normalized specular intensity is plotted using blue circular markers, and decays continuously as a function of exposure. The normalized intensity at the first order diffraction pattern along the $\langle 110 \rangle$ crystal azimuth is plotted using red square markers. The diffraction signal increases gradually with exposure and peaks at an exposure which attenuates the specular intensity by $\sim \times 20$. Further exposure reduces the diffraction signal intensity, indicating the growth of a multilayer amorphous solid water layer.

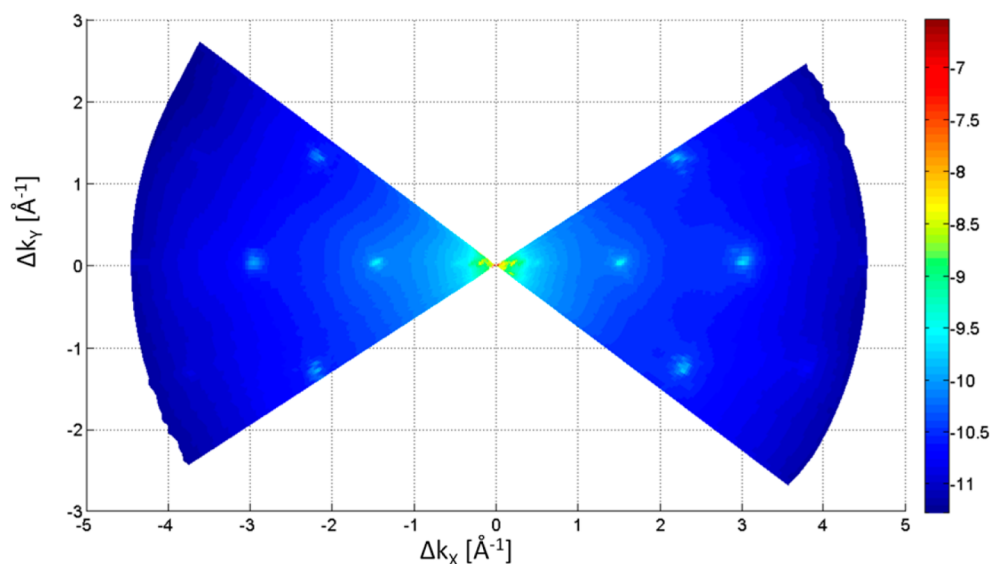


Figure 3. 2D color plot of the logarithm of the scattered helium intensity as a function of parallel momentum transfer performed using a 12 meV ^3He beam. The H₂O layer was grown at 110 K under the optimal exposure conditions described in the text. The image was obtained by combining 71 in-plane 1D angular scans (of the type shown in Figure 1) performed for different crystal azimuth angles. The $\langle 110 \rangle$ azimuth is oriented along the horizontal axis of the plot. Eight strong and sharp diffraction features can be seen in the high symmetry directions, whereas additional weaker peaks can be resolved for larger momentum transfer values in between the high symmetry directions. In addition to the characteristic herringbone peaks seen close to the origin ($\Delta K = 0$), some very faint satellite peaks appear to be surrounding the main diffraction peaks along the diagonal azimuth, while the limited resolution and signal-to-noise ratio of the measurement do not allow a detailed analysis of these peaks, their approximate position is also in agreement with the expected herringbone reconstruction pattern.²⁷

RESULTS AND DISCUSSION

Figure 1 shows the evolution of HAS angular scans along the $\langle 110 \rangle$ crystal azimuth as a function of the H₂O coverage. The measurements were performed by monitoring the scattered helium intensity while rotating the surface normal within the scattering plane and converting the scattering angle to the momentum transfer parallel to the surface, denoted as ΔK . The sample temperature was 110 K during both the overlayer

growth and the HAS measurements. For the clean Au(111), we observe a sharp specular peak surrounded by the satellite peaks of the herringbone reconstruction, as was seen in previous HAS experiments.²⁷ Other diffraction features which were observed on the clean surface were weak first order peaks positioned along the $\langle 112 \rangle$ crystal azimuth (data not shown), which are also in agreement with the herringbone reconstruction pattern.²⁷ While exposing the surface to water, the intensity

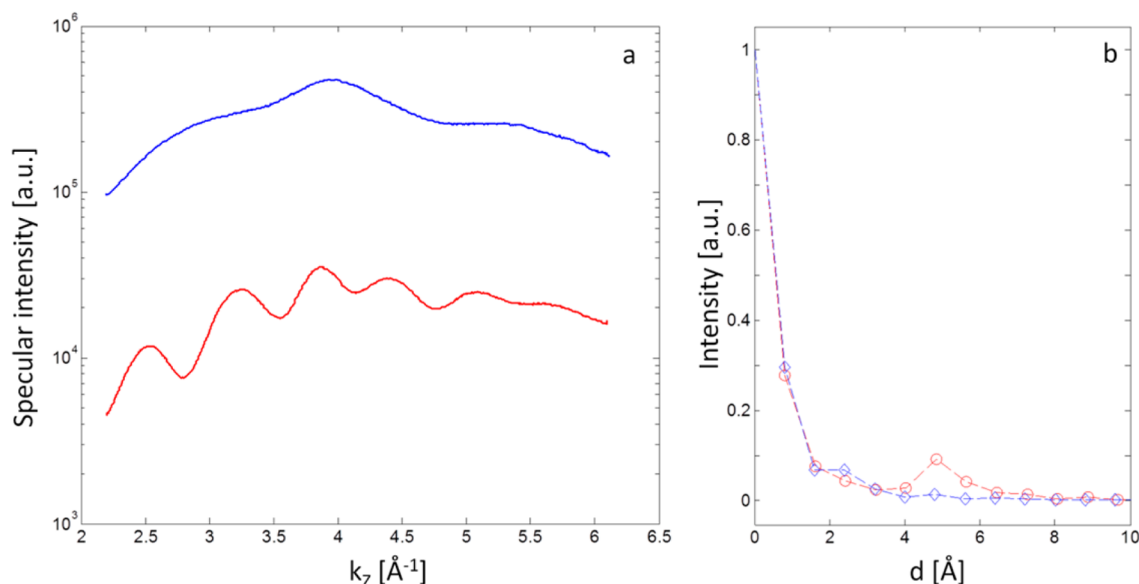


Figure 4. (a) Specular signal intensity as a function of the perpendicular component of the helium beam wave vector. Measurements were performed by changing the energy of a ^4He beam between 2.9 and 23 meV. The surface temperature for both the clean Au(111) (blue) and the $\text{H}_2\text{O}/\text{Au}(111)$ (red) measurements was 110 K, the H_2O layer was produced using the optimal diffraction conditions mentioned in the text above. (b) Normalized Fourier transforms of the curves shown in the left panel (blue diamonds and red circles correspond to clean and H_2O covered surfaces). The horizontal scale plots the angular frequency divided by two, which corresponds to the height difference, d , between the interfering surfaces. The resolution within which d can be determined is governed by the total range of k_z values measured in the experiment.

of the specular peak quickly decreases (the legend indicates the specular signal attenuation for each scan presented in the figure), and concurrently first and second order diffraction peaks emerge with a spacing of $\Delta K = 1.49 \pm 0.03 \text{ \AA}^{-1}$.²⁸ The intensity of these diffraction peaks initially increases; however, longer exposures lead to a reduction in intensity and eventually to the disappearance of the diffraction peaks (dose > 10 L), resulting in a broad featureless distribution as would be expected for an amorphous surface.¹⁰ Figure 2 shows the evolution of the scattered signal from both the specular scattering condition and the first order peak along the $\langle 110 \rangle$ crystal azimuth as a function of H_2O exposure. Two features that can be seen in the figure are (1) a gradual increase of the diffraction signal with coverage, consistent with an island growth mode and (2) the existence of a maximum in the diffraction intensity, which occurs when the specular signal reduces by a factor of approximately 20 with respect to the intensity of the clean surface, the actual exposures needed to obtain the maximal diffraction signal intensity were sample dependent.²⁹ A further point to note is that with increasing exposure beyond that at which the maximum in the diffraction intensity is reached, the intensities of the first- and second-order diffraction peaks decrease together at approximately the same rate. This rate is significantly smaller than the concomitant decrease in the specular intensity. That the attenuation rates of the first- and second-order diffraction peaks are similar is expected according to a Debye–Waller model for disorder³¹ because the total momentum transfer is dominated by the perpendicular component, which does not vary significantly between the two. In contrast, the much stronger attenuation of the specular peak suggests that its intensity is related to contributions from both the water-covered regions of the surface as well as bare Au(111) regions, which coexist on the surface, an issue that we discuss in more detail below.

Figure 3 shows a 2D angular scan obtained by repeating angular scans of the type shown in Figure 1 for different crystal

azimuths (i.e., rotating the sample about the surface normal between each angular scan) and plotting the logarithm of the measured scattered signal intensity. The temperature of the sample during the layer growth and measurement was 110 K, the H_2O exposure was stopped when the specular signal reduced by a factor of 20 corresponding to the optimal conditions of the diffraction peak mentioned above. In addition to the sharp specular peak surrounded by the herringbone satellite peaks (seen more clearly in the 1D measurements plotted in Figure 1), the measurement shows a well-ordered diffraction pattern of the H_2O overlayer.

The positions of the relatively sharp diffraction spots seen in our measurements are very close to those expected from a $(\sqrt{3} \times \sqrt{3})R30^\circ$ structure on the Au(111) surface (our measured peaks correspond to a structure that is compressed by less than 3% with respect to the bulk terminated surface); hence, given our experimental uncertainty, the structure we measure can be considered as commensurate with the gold surface. Thus, as opposed to what one might expect, the weak H_2O –Au interactions do not prevent the growth of an ordered compact H_2O structure which maintains a high degree of order and commensurability at relatively high temperatures. In fact, a further increase in the intensity of the first order diffraction peak intensity was observed when growing the layer at 130 K (see Figure S2 in the Supporting Information). In contrast, the diffraction peak completely vanishes at 140 K, a temperature that is close to the crystallization transition in bulk ice, and to a transition observed on Cu(111) where relatively flat H_2O islands turn into corrugated pyramid-like structures.⁶

The fact that the herringbone reconstruction that characterizes the clean surface can be seen alongside the $(\sqrt{3} \times \sqrt{3})R30^\circ$ diffraction pattern could be interpreted as an indication that water does not lift the Au(111) reconstruction; however, the persistence of the pattern may also be simply related to the fact that the surface is only partially covered with water, leaving exposed regions of the reconstructed Au(111) surface. As

explained below, the measurements presented in Figure 4 lead us to believe that the surface is in fact only partially covered under the conditions of our experiment.

Figure 4a shows the intensity of the helium specular reflection as a function of the perpendicular component of the wave vector, which was scanned by heating the nozzle from 13.6 K (2.9 meV) to 106 K (23 meV) while maintaining specular conditions, that is, without exchanging momentum within the surface plane. This type of measurement can be used to detect and study surface structures that exhibit order in the direction perpendicular to the surface plane or, alternatively, to study the helium–surface interaction with high precision.³² An overall trend seen for both the clean and H₂O covered surface is an initial increase in intensity followed by a slow reduction at higher wave vector values, reflecting the source intensity dependencies and the Debye–Waller factor. Additional features are the oscillating patterns seen in both curves, a faint oscillation with a period of $\sim 1.3 \text{ \AA}^{-1}$ for the clean Au(111) surface, and a pronounced oscillation with a period of 0.63 \AA^{-1} after deposition of H₂O.

For specular conditions, an oscillation pattern is expected when the surface is characterized by flat regions with a well-defined height difference. In this case, constructive interference is expected when the height between the two surfaces, d , satisfies the relation $k_z d = n\pi$. Therefore, the oscillations we observe on the clean surface correspond to a d value of approximately 2.4 Å, which is quite close to the expected height difference (2.5 Å) between Au(111) terraces separated by a single-atom height step. The higher frequency seen in the red curve indicates that the growth of H₂O leads to interference between surfaces with a substantially larger height difference of $\sim 5 \text{ \AA}$. Figure 4b shows an alternative method of extracting the heights from the measurements. This plot shows the Fourier transform of the curves shown in Figure 4a, where the horizontal scale shows the angular frequency divided by 2, which should correspond to the height difference, d . A faint peak at $\sim 2.5 \text{ \AA}$ and a clear peak at $\sim 5 \text{ \AA}$ can be seen for the clean and H₂O covered surfaces, respectively.

The data presented in Figure 4 indicates that under the same conditions where the optimal diffraction pattern is obtained we do not have complete wetting of the surface with a single water layer, as this would maintain the topography of the underlying gold surface and should not alter the oscillation period. This finding is consistent with the low temperature observations of partial dewetting on Cu(111)⁶ given the fact that the H₂O–Au(111) interaction is assumed to be even weaker than that of H₂O–Cu(111).¹⁴ Hence, the oscillation pattern seen after water deposition, reflects interference effects between bare Au(111) regions and the surface of H₂O islands which are characterized by a uniform height of approximately 5 Å. This height value supports the proposition of a double bilayer H₂O structure on Au(111)¹⁷ and is approximately 20% lower than the DFT calculation performed on this system.³³ Our height value is also not too different (approximately 25% lower) with respect to the value deduced from STM measurements of the double bilayer structures observed on Cu(111).⁶ The fact that we do not observe larger-periodicity oscillations after exposing the surface to H₂O indicates that if both single and double bilayer islands coexist on the surface at our experimental conditions, the relative fraction of the single bilayer islands is significantly smaller than that of the double bilayer islands.

It is important to note that strictly speaking height estimations from oscillation curves should take into account

the differences in the attractive part of the helium–surface interaction potential between the clean and the H₂O covered part of the surface, as well as a shift of the repulsive part of the potential due to a different decay rate of the electron density into the vacuum. Unfortunately, we are not aware of any reliable potentials for He/H₂O/Au(111), which would allow to perform such an analysis. Nevertheless, past experience shows that the errors anticipated from neglecting the details of the scattering potential³² are not expected to be larger than the experimental uncertainty of our height values, which is dictated by the restricted number of oscillations we can measure and approximated as $\sim 0.5 \text{ \AA}$. Finally, the lateral size of the ordered ice structures can also be estimated from the relatively narrow width of the first order diffraction peaks at the optimal growth conditions (FWHM $< 0.09 \text{ \AA}^{-1}$), yielding an estimate of 70 Å for the lateral extent of the well-ordered surface patches. We did not observe any significant change in this value after further ($\times 3$) H₂O exposure even though further exposure significantly reduces the diffraction peak height.³⁴

While the observations presented above indicate long-range order with a particular symmetry and unit cell size, there are several questions that will need to be addressed in order to understand the exact real space structure of this system. One initial question is whether an ordered helium diffraction necessarily implies that the layer is proton ordered or not. On the one hand, HAS is not always guaranteed to detect proton order as has been shown by Glebov et al. for the surface of crystalline ice.¹⁰ Glebov et al. showed that both a proton ordered model and an alternative model, which includes a (relatively small) corrugation due to disordered protons, can be used to reproduce their experimental data. On the other hand, HAS is known to be very sensitive to light atoms and the structure of H-atoms on a clean surface has been studied in detail.³⁵ There is also growing evidence that HAS is sensitive to proton order in H₂O surfaces. In particular, Gallagher et al. showed that the sensitivity of helium to proton order can explain the apparent discrepancy between the LEED and HAS results on H₂O/Ru(0001).³⁶ Furthermore, evidence for the sensitivity of HAS to proton order has been shown in a recent study of a H₂O layer on an oxygen precovered Ru(0001) surface,¹² where the measured diffraction pattern was characterized by a glide line, demonstrating the sensitivity to the internal structure within the unit cell, that is, the proton order. Thus, while HAS is definitely sensitive to hydrogen atoms, and can detect proton order on certain systems, the relation between a HAS diffraction pattern and proton-order needs to be assessed individually for any specific surface system. In particular, in systems of the type reported in this work, where there are no obvious missing diffraction spots indicating internal structure, further experimental support from other independent measurement techniques or detailed scattering calculations (when these can be reliably performed) are needed to relate the diffraction pattern and the proton order with confidence.

Regardless of whether the surface is proton ordered or not, the compact unit cell we observe is very different from the large unit cells seen on Pt(111) and Ni(111).^{21,37} The compact commensurate structure we observe on Au(111) cannot be simply explained using geometrical considerations, as the gold surface does not provide better lattice matching than Pt(111) or Ni(111). Another interesting comparison is with Ru(0001), here one could naively expect that the close geometrical match and the strong interaction could lead to a well-ordered bilayer

model. Nevertheless, previous measurements have shown that even though the oxygens adopt the $(\sqrt{3} \times \sqrt{3})R30^\circ$ pattern, the lack of a clear helium scattering diffraction pattern suggests a disordered surface.³⁶ It is possible that the mechanism that leads to the ordered structure and compact unit cell we observe on Au(111) is linked with the fact that the water islands seem to grow as two layer high structures, unlike what is seen on more reactive surfaces. The structural model introduced by Stacchiola et al. (Figure S1 in the Supporting Information) provides a structure that is consistent with our measurements in terms of symmetry, commensurability, and height; nevertheless, further experiments and elaborate scattering calculations are needed to validate this model, especially due to the considerable challenges encountered when performing DFT calculations of water surfaces in general and on Au(111), in particular.^{5,38}

Common aspects can be found when comparing our results with STM studies on another weakly interacting system, H₂O/Cu(111), in particular, the partial dewetting mentioned earlier and the growth of double bilayer high H₂O islands.⁶ On the other hand, our measurements suggest long-range order within the surface of the H₂O islands, whereas the STM results, performed after annealing to 118 K and cooling back to imaging temperatures, indicate an amorphous structure for the surface of the islands. Obviously, these differences could be attributed to the variations between the copper and gold surfaces; however, they could also be a result of the different experimental probes used, in particular, the different sensitivity to surface motion and perturbation effects for STM and HAS. Finally, ordered structures of H₂O/Cu(111) were seen with the STM when the surface was annealed to higher temperatures (140 K).⁶ These pyramidal four-layer-high structures developed at the temperatures of the amorphous to crystalline transition, and due to their heterogeneous appearance and highly corrugated surfaces would not be expected to provide a sharp helium diffraction of the type we measured. Hence, if these types of islands develop on Au(111) at similar temperatures, they might explain why we observed a disappearance of the diffraction pattern after annealing to 140 K.

CONCLUSIONS

In summary, using helium atom scattering we observe the formation of a water layer on Au(111). This layer is characterized by highly commensurate long-range ordered structures with a $(\sqrt{3} \times \sqrt{3})R30^\circ$ symmetry, which grow as islands with a height of approximately 5 Å. These findings provide support for the “double-bilayer” structure suggested recently for this system.¹⁷ The ordered structures are observed at relatively high temperatures (up to 130 K) and vanish only when the crystal is annealed at temperatures approaching the amorphous-to-crystalline transition of bulk ice. The high degree of order is surprising given other independent observations, in particular the notoriously weak Au–H₂O interaction, the amorphous nature of H₂O islands imaged with high resolution on Cu(111), and the amorphous structure observed on the much more reactive Ru(0001) surface.³⁶ One possible explanation is that the herringbone reconstruction of the Au(111) plays a special role in establishing order within the H₂O layers, other explanations might be due to the different experimental probes used. Further comparative studies are needed to answer these questions.

ASSOCIATED CONTENT

Supporting Information

A description of the double bilayer model, experimental details, and a comparison of the diffraction peak intensity at different growth temperatures. This material is available free of charge via the Internet at <http://pubs.acs.org>.

AUTHOR INFORMATION

Corresponding Author

*E-mail: ga232@tx.technion.ac.il.

Present Address

[§]Shell Upstream International, Schepersmaat 2, 9405 TA Assen, The Netherlands (P.R.K.).

Author Contributions

[†]These authors contributed equally (G.C. and P.R.K.).

Notes

The authors declare no competing financial interest.

ACKNOWLEDGMENTS

The authors would like to thank Dr. J. Ellis and Dr. W. Allison from the Cavendish Laboratory for generously providing access to their spectrometer, Prof. H. Ibach for helpful discussions and Dr. Ping Liu and Dr. Dario Stacchiola from the Brookhaven National Laboratory who kindly provided us the details of their DFT results. J.R.M. would like to acknowledge the generous hospitality of the Chemistry Department of the Technion. This work was funded by the European Research Council under the European Union's seventh framework program (FP/2007–2013)/ ERC Grant 307267, the United States-Israel Binational Science Foundation, Grant 2010095, and the German-Israeli Foundation for Scientific Research and Development.

REFERENCES

- (1) Hendersson, M. A. The Interaction of Water With Solid Surfaces: Fundamental Aspects Revisited. *Surf. Sci. Rep.* **2002**, *46*, 1–308.
- (2) Hodgson, A.; Haq, S. Water Adsorption and the Wetting of Metal Surfaces. *Surf. Sci. Rep.* **2009**, *64* (9), 381–451.
- (3) Verdager, A.; Sacha, G. M.; Bluhm, H.; Salmeron, M. Molecular Structure of Water at Interfaces: Wetting at the Nanometer Scale. *Chem. Rev.* **2006**, *106* (4), 1478–1510.
- (4) Feibelman, P. J. The First Wetting Layer on a Solid. *Phys. Today* **2010**, *63* (2), 34–39.
- (5) Carrasco, J.; Santra, B.; Klimes, J.; Michaelides, A. To Wet or Not to Wet? Dispersion Forces Tip the Balance for Water Ice on Metals. *Phys. Rev. Lett.* **2011**, *106* (2), 026101.
- (6) Mehlhorn, M.; Morgenstern, K. Height Analysis of Amorphous and Crystalline Ice Structures on Cu(111) in Scanning Tunneling Microscopy. *New J. Phys.* **2009**, *11*, 093015.
- (7) Carrasco, J.; Michaelides, A.; Forster, M.; Haq, S.; Raval, R.; Hodgson, A. A One-Dimensional Ice Structure Built From Pentagons. *Nat. Mater.* **2009**, *8* (5), 427–431.
- (8) Gawronski, H.; Morgenstern, K.; Rieder, K. H. Electronic Excitation of Ice Monomers on Au(111) by Scanning Tunneling Microscopy. *Eur. Phys. J. D* **2005**, *35* (2), 349–353.
- (9) Glebov, A.; Graham, A. P.; Menzel, A.; Toennies, J. P. Orientational Ordering of Two-Dimensional Ice on Pt(111). *J. Chem. Phys.* **1997**, *106* (22), 9382–9385.
- (10) Glebov, A.; Graham, A. P.; Menzel, A.; Toennies, J. P.; Senet, P. A Helium Atom Scattering Study of the Structure and Phonon Dynamics of the Ice Surface. *J. Chem. Phys.* **2000**, *112*, 11011.
- (11) Gibson, K. D.; Viste, M.; Sibener, S. J. The Adsorption of Water on Clean and Oxygen Predosed Rh(111): Surface Templating via (1×1) -O/Rh(111) Induces Formation of a Novel High-Density Interfacial Ice Structure. *J. Chem. Phys.* **2000**, *112* (21), 9582–9589.

(12) Avidor, N.; Hedgeland, H.; Held, G.; Jardine, A. P.; Allison, W.; Ellis, J.; Kravchuk, T.; Alexandrowicz, G. Highly Proton-Ordered Water Structures on Oxygen Precovered Ru{0001}. *J. Phys. Chem. A* **2011**, *115* (25), 7205–7209.

(13) Michaelides, A.; Ranea, V. A.; de Andres, P. L.; King, D. A. General Model for Water Monomer Adsorption on Close-Packed Transition and Noble Metal Surfaces. *Phys. Rev. Lett.* **2003**, *90* (21), 216102.

(14) Carrasco, J.; Klimes, J.; Michaelides, A. The Role of van der Waals Forces in Water Adsorption on Metals. *J. Chem. Phys.* **2013**, *138* (2), 024708.

(15) Scott Smith, R.; Huang, C.; Wong, E. K. L.; Kay, B. D. Desorption and Crystallization Kinetics in Nanoscale Thin Films of Amorphous Water Ice. *Surf. Sci.* **1996**, *367* (1), L13–L18.

(16) Ikemiya, N.; Gewirth, A. A. Initial Stages of Water Adsorption on Au Surfaces. *J. Am. Chem. Soc.* **1997**, *119* (41), 9919–9920.

(17) Stacchiola, D.; Park, J. B.; Liu, P.; Ma, S.; Yang, F.; Starr, D. E.; Muller, E.; Sutter, P.; Hrbek, J. Water Nucleation on Gold: Existence of a Unique Double Bilayer. *J. Phys. Chem. C* **2009**, *113* (34), 15102–15105.

(18) Ibach, H. Electron Energy Loss Spectroscopy of the Vibration Modes of Water on Ag(100) and Ag(115) Surfaces and Comparison to Au(100), Au(111) and Au(115). *Surf. Sci.* **2012**, *606* (19–20), 1534–1541.

(19) Pirug, G.; Bonzel, H. P. UHV Simulation of the Electrochemical Double Layer: Adsorption of HClO₄/H₂O on Au(111). *Surf. Sci.* **1998**, *405* (1), 87–103.

(20) Morgenstern, M.; Muller, J.; Michely, T.; Comsa, G. The Ice Bilayer on Pt(111): Nucleation, Structure and Melting. *Z. Phys. Chem* **1997**, *198*, 43–72.

(21) Standop, S.; Redinger, A.; Morgenstern, M.; Michely, T.; Busse, C. Molecular Structure of the H₂O Wetting Layer on Pt(111). *Phys. Rev. B* **2010**, *82*, 161412.

(22) Nie, S.; Feibelman, P. J.; Bartelt, N. C.; Thurmer, K. Pentagons and Heptagons in the First Water Layer on Pt(111). *Phys. Rev. Lett.* **2010**, *105* (2), 026102.

(23) Carrasco, J.; Hodgson, A.; Michaelides, A. A Molecular Perspective of Water at Metal Interfaces. *Nat. Mater.* **2012**, *11* (8), 667–674.

(24) Fouquet, P.; Jardine, A. P.; Dworski, S.; Alexandrowicz, G.; Allison, W.; Ellis, J. Thermal Energy ³He Spin-Echo Spectrometer for Ultrahigh Resolution Surface Dynamics Measurements. *Rev. Sci. Instrum.* **2005**, *76* (5), 053109–13.

(25) Alexandrowicz, G.; Jardine, A. P. Helium Spin-Echo Spectroscopy: Studying Surface Dynamics with Ultra-High-Energy Resolution. *J. Phys. Condens. Matter* **2007**, *19* (30), 305001.

(26) In order to calibrate the exposure, we performed experiments with both an indirect dose and the capillary array and determined the ratio of the pressure readings which give rise to a similar reduction of specular intensity.

(27) Harten, U.; Lahee, A. M.; Toennies, J. P.; Woll, C. Observation of a Soliton Reconstruction of Au(111) by High-Resolution Helium-Atom Diffraction. *Phys. Rev. Lett.* **1985**, *54* (24), 2619–2622.

(28) The two main contributions to the experimental uncertainty are the width of the energy distribution of the incident helium beam (0.2 meV HWHM), and sample misalignment. A brief description of the method for measuring the energy distribution is given in the supplementary online information.

(29) The exact dose that led to a specular attenuation of ×20 and a maximum in the diffraction signal changed between 0.7 and 3 L for the two different Au(111) crystals used in this study. The crystal that required larger exposures to achieve the ×20 specular attenuation had a slightly lower specular reflectivity value of 15% (vs 20% for the second crystal), which could indicate a larger step density. Because the decoration of steps by adsorbates leads to a reduced specular attenuation with respect to covering flat terraces, larger exposures are needed to reduce the specular attenuation in comparison with a flat surface. Furthermore, step densities and their relation to coadsorption

phenomena have been shown to strongly influence H₂O structure in a recent STM study on Pt(111).³⁰

(30) Standop, S.; Morgenstern, M.; Michely, T.; Busse, C. H₂O on Pt(111): Structure and Stability of the First Wetting Layer. *J. Phys.: Condens. Matter* **2012**, *24*, 124103.

(31) Garcia, N.; Celli, V.; Nietovesperinas, M. Exact Multiple-Scattering of Waves from Random Rough Surfaces. *Opt. Commun.* **1979**, *30* (3), 279–281.

(32) Ellis, J.; Hermann, K.; Hofmann, F.; Toennies, J. P. Experimental Determination of the Turning Point of Thermal Energy Helium Atoms above a Cu(001) Surface. *Phys. Rev. Lett.* **1995**, *75* (5), 886–889.

(33) Private correspondence. Dr. P. Liu, Brookhaven National Laboratory.

(34) Such behavior would be expected if the additional H₂O exposure covers some of the ordered water islands with an additional disordered layer which scatters diffusely and does not contribute to the diffraction pattern. In this case the residual diffraction signal reflects the diminishing number of islands which were still unaffected by the further growth and therefore maintain the same coherence length and corresponding peak width.

(35) Graham, A. P.; Fang, D.; McCash, E. M.; Allison, W. Adsorption of Atomic Hydrogen on Cu(001) Studied with Helium-Atom Scattering. *Phys. Rev. B* **1998**, *57* (20), 13158–13166.

(36) Gallagher, M.; Omer, A.; Darling, G. R.; Hodgson, A. Order and Disorder in the Wetting Layer on Ru(0001). *Faraday Discuss.* **2009**, *141*, 231–249.

(37) Gallagher, M. E.; Haq, S.; Omer, A.; Hodgson, A. Water Monolayer and Multilayer Adsorption on Ni(111). *Surf. Sci.* **2007**, *601* (1), 268–273.

(38) Hanke, F.; Bjork, J. Structure and Local Reactivity of the Au(111) Surface Reconstruction. *Phys. Rev. B* **2013**, *87* (23), 235422.